

STIM1, PKC- δ and RasGRP set a threshold for proapoptotic Erk signaling during B cell development

Andre Limnander¹, Philippe Depeille², Tanya S Freedman¹, Jen Liou³, Michael Leitges^{4,5}, Tomohiro Kurosaki^{6,7}, Jeroen P Roose² & Arthur Weiss¹

Clonal deletion of autoreactive B cells is crucial for the prevention of autoimmunity, but the signaling mechanisms that regulate this checkpoint remain undefined. Here we characterize a previously unrecognized Ca²⁺-driven pathway for activation of the kinase Erk, which was proapoptotic and biochemically distinct from Erk activation induced by diacylglycerol (DAG). This pathway required protein kinase C- δ (PKC- δ) and the guanine nucleotide-exchange factor RasGRP and depended on the concentration of the Ca²⁺ sensor STIM1, which controls the magnitude of Ca²⁺ entry. Developmental regulation of these proteins was associated with selective activation of the pathway in B cells prone to negative selection. This checkpoint was impaired in PKC- δ -deficient mice, which developed B cell autoimmunity. Conversely, overexpression of STIM1 conferred a competitive disadvantage to developing B cells. Our findings establish Ca²⁺-dependent Erk signaling as a critical proapoptotic pathway that mediates the negative selection of B cells.

Early B cell development in the bone marrow is characterized by rearrangements of the immunoglobulin locus that lead to the production of a unique B cell antigen receptor (BCR) on the surface of each B cell. This process generates an exceptionally diverse repertoire of B cells for the recognition of potential foreign invaders. However, a sizeable portion of the initial repertoire has the ability to recognize self, and these cells must be modified, silenced or eliminated to prevent later autoimmunity^{1–5}. Immature bone marrow B cells initially express the BCR as membrane-bound immunoglobulin M (IgM), which establishes the first opportunity for the cells to recognize antigen. Antigen engagement at this stage results in upregulation of the recombination machinery and receptor editing, one way by which autoreactivity can be avoided while the cell is rescued⁶. However, as cells progress through development and continue increasing their surface abundance of IgM and IgD, they lose the ability to edit the receptor and instead become increasingly sensitive to antigen-induced apoptosis⁷. These transitional bone marrow cells thus undergo apoptosis after encountering antigen, a second checkpoint that prevents the development of later autoimmunity. Cells that survive past this stage then leave the bone marrow and migrate to the spleen, where they undergo additional selection checkpoints before completing maturation. Once B cells reach a mature stage, they become resistant to antigen-induced apoptosis and instead mount vigorous proliferative responses to antigen. Therefore, developmental changes during B cell maturation alter signaling responses to antigen in ways that lead to different functional

outcomes. The molecular mechanisms by which antigen encounter leads to editing, apoptosis or proliferation at different stages of B cell development are not well understood.

Developing B cells produce less diacylglycerol (DAG) and show greater amplitude and duration of Ca²⁺ entry in response to antigen, particularly at low antigen concentrations, than do mature B cells^{8–11}. Ca²⁺ is essential for both receptor editing and antigen-induced apoptosis⁷, which indicates that greater amplitude of the entry of Ca²⁺ into developing B cells probably contributes to their greater sensitivity to antigen-induced apoptosis. The mechanism that drives Ca²⁺ into a lymphocyte is initiated by depletion of intracellular stores: crosslinking of the antigen receptor leads to activation of phospholipase C- γ , which converts phosphatidylinositol-(4,5)-bisphosphate into inositol-(1,4,5)-trisphosphate and DAG; inositol-(1,4,5)-trisphosphate then binds to its receptors on the endoplasmic reticulum membrane, which leads to depletion of Ca²⁺ from the endoplasmic reticulum stores. This triggers an initial increase in the cytoplasmic Ca²⁺ concentration, followed by opening of the Ca²⁺ release-activated Ca²⁺ channels (or other store-operated Ca²⁺ channels, such as TRP channels, depending on the cell type) at the plasma membrane. Extracellular Ca²⁺ then flows into the cell following a 10,000-fold gradient and further prolongs the increases in intracellular Ca²⁺ concentration, a process known as 'store-operated Ca²⁺ entry' (SOCE)¹². The mechanism that couples the release of endoplasmic reticulum stores to opening of the plasma membrane channels has been defined, in part due to

¹Department of Medicine, Howard Hughes Medical Institute, Rosalind Russell Medical Research Center for Arthritis, University of California at San Francisco, San Francisco, California, USA. ²Department of Anatomy, University of California at San Francisco, San Francisco, California, USA. ³Department of Physiology, University of Texas Southwestern Medical Center, Dallas, Texas, USA. ⁴Division of Nephrology, Department of Medicine, Hannover Medical School, Hannover, Germany. ⁵The Biotechnology Centre of Oslo, University of Oslo, Oslo, Norway. ⁶Laboratory for Lymphocyte Differentiation, World Premier International Immunology Frontier Research Center, Osaka University, Osaka, Japan. ⁷Laboratory for Lymphocyte Differentiation, RIKEN Research Center for Allergy and Immunology, Yokohama, Japan. Correspondence should be addressed to A.W. (aweiss@medicine.ucsf.edu).

Received 7 February; accepted 2 March; published online 27 March 2011; doi:10.1038/ni.2016

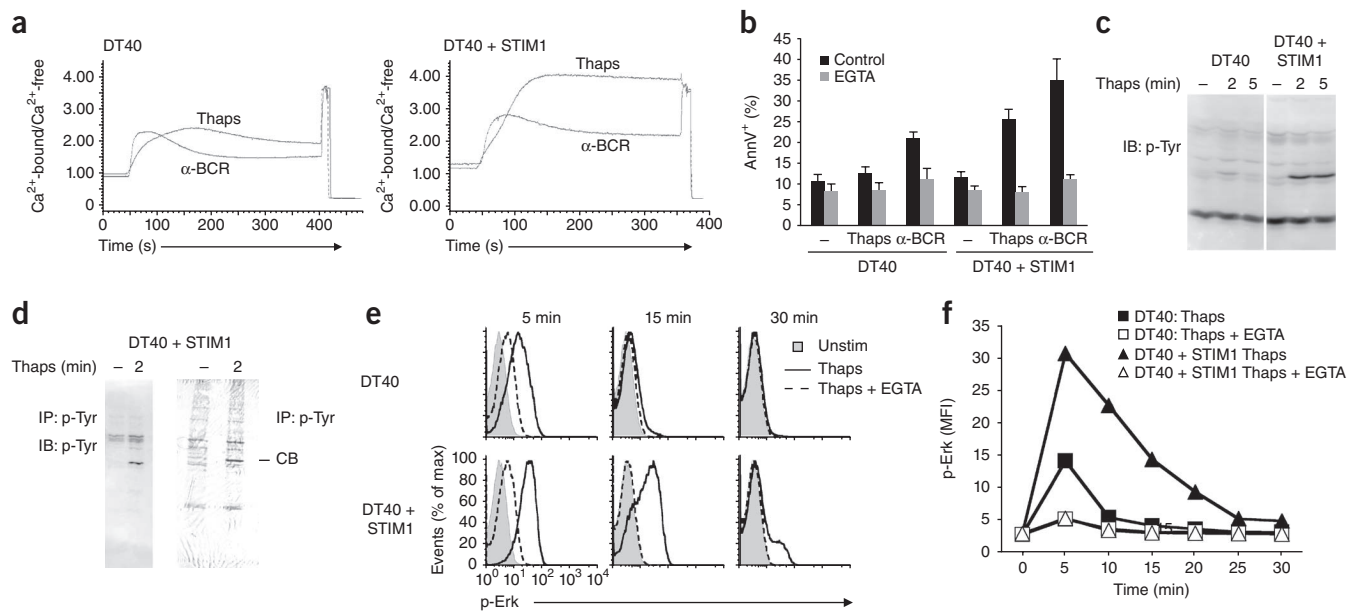


Figure 1 Sensitization of B cells to antigen-induced apoptosis correlates with Ca²⁺-dependent activation of Erk. **(a)** Intracellular Ca²⁺ in wild-type DT40 cells (DT40; left) and DT40 cells overexpressing STIM1 (DT40 + STIM1; right) stimulated with 1 μM thapsigargin (Thaps) or M4 antibody to the BCR (α-BCR), followed by lysis (maximum Ca²⁺-bound emissions) for termination of stimulation, and Ca²⁺ chelation with EGTA (maximum Ca²⁺-free emissions). **(b)** Annexin V (AnnV) staining on the surface of cells left unstimulated (–) or stimulated for 8 h as in **a**. **(c)** Immunoblot analysis (IB) of lysates of cells left unstimulated or stimulated for 2 or 5 min (above lanes) with thapsigargin, probed with antibodies 4G10 and RC20 to phosphorylated tyrosine (p-Tyr). **(d)** Immunoprecipitation (with 4G10) of proteins containing phosphorylated tyrosine from lysates of unstimulated or thapsigargin-stimulated cells, followed by SDS-PAGE and immunoblot analysis (left) or staining with colloidal blue (CB; right); arrow indicates band excised and identified as Erk2 by mass spectrometry. **(e)** Flow cytometry of thapsigargin-stimulated cells, assessing the intensity of phosphorylated Erk. **(f)** Mean fluorescence intensity (MFI) of the phosphorylated Erk in **e**, over time. Data are representative of at least five experiments each (**a–c,e,f**; error bars (**b**), s.e.m.) or one experiment (**d**).

the identification of STIM1 as the long-sought Ca²⁺ sensor in the endoplasmic reticulum^{13–15}. STIM1 is a transmembrane endoplasmic reticulum protein that contains a Ca²⁺-binding EF hand located in the lumen of the endoplasmic reticulum. Under resting conditions, STIM1 is Ca²⁺ bound and evenly distributed through the endoplasmic reticulum membrane. After release of the endoplasmic reticulum Ca²⁺ stores, STIM1 becomes unbound from Ca²⁺ and clusters and moves toward the plasma membrane, where it interacts with the channels^{16–20}, causing them to open and triggering the entry of extracellular Ca²⁺. STIM1 is thus essential for SOCE, but the extent to which the abundance of STIM1 protein influences the potential magnitude of Ca²⁺ responses has not been explored.

Here we use STIM1 to establish a system for sensitization of B cells to antigen receptor-induced apoptosis. With this system we identify and characterize a previously unrecognized Ca²⁺-driven pathway involved in activation of the kinase Erk. We demonstrate that STIM1 overexpression in a B cell line augmented the amplitude and duration of Ca²⁺ entry and enhanced antigen receptor-induced apoptosis. By mass spectrometry we identify a Ca²⁺-dependent pathway to Erk with biochemical requirements distinct from those for DAG-mediated activation of Erk. Activation of this Ca²⁺-dependent pathway required the activity of the guanine nucleotide-exchange factor RasGRP and protein kinase C-δ (PKC-δ), and its disruption rescued the cells from antigen receptor-induced apoptosis. Furthermore, we identify Ser332 on human RasGRP1 as a potential phosphorylation site that is a likely target for PKC-δ and was essential for activation of this Ca²⁺-Erk pathway. Primary bone marrow B cells prone to negative selection had differences in their expression of STIM1, PKC-δ and RasGRP, and as a result, this pathway was selectively activated in these

B cell subsets. PKC-δ-deficient developing B cells failed to activate this pathway, which correlated with the development of self-reactive B cells and autoimmunity in these mice^{21,22}. In contrast, developing B cells overexpressing STIM1 showed more negative selection at the bone marrow transitional stage, and this effect required PKC-δ. Our findings demonstrate that DAG and Ca²⁺ can direct Erk signaling toward different functional outcomes, thus outlining a molecular mechanism by which developmental regulation of Ca²⁺- and DAG-dependent Erk pathways can determine B cell fate.

RESULTS

STIM1 increases SOCE and apoptosis in DT40 B cells

Published work has described a role for STIM1 in SOCE^{13–15}. We hypothesized that STIM1 might act as the limiting factor in controlling the rate of the opening of Ca²⁺ release-activated Ca²⁺ channels and thus control the induction of apoptosis. Indeed, cells of the DT40 chicken B cell line stably overexpressing STIM1 tagged with enhanced yellow fluorescent protein (eYFP-STIM1; **Supplementary Fig. 1**) had a greater amplitude and duration of SOCE than did wild-type DT40 cells in response to stimulation of the BCR or treatment with thapsigargin or cyclopiazonic acid (CPA; **Fig. 1a** and **Supplementary Fig. 2a**). Thapsigargin and CPA trigger SOCE by inhibiting the sarcoplasmic-endoplasmic reticulum Ca²⁺-ATPase pumps in the endoplasmic reticulum, thereby inducing passive release of Ca²⁺ from the endoplasmic reticulum stores while bypassing proximal BCR signaling. Consistent with a role for Ca²⁺ in antigen-induced apoptosis^{8,10}, overexpression of STIM1 sensitized DT40 cells to both BCR-induced apoptosis and thapsigargin-induced apoptosis (**Fig. 1b**). Furthermore, chelation of extracellular Ca²⁺ with EGTA

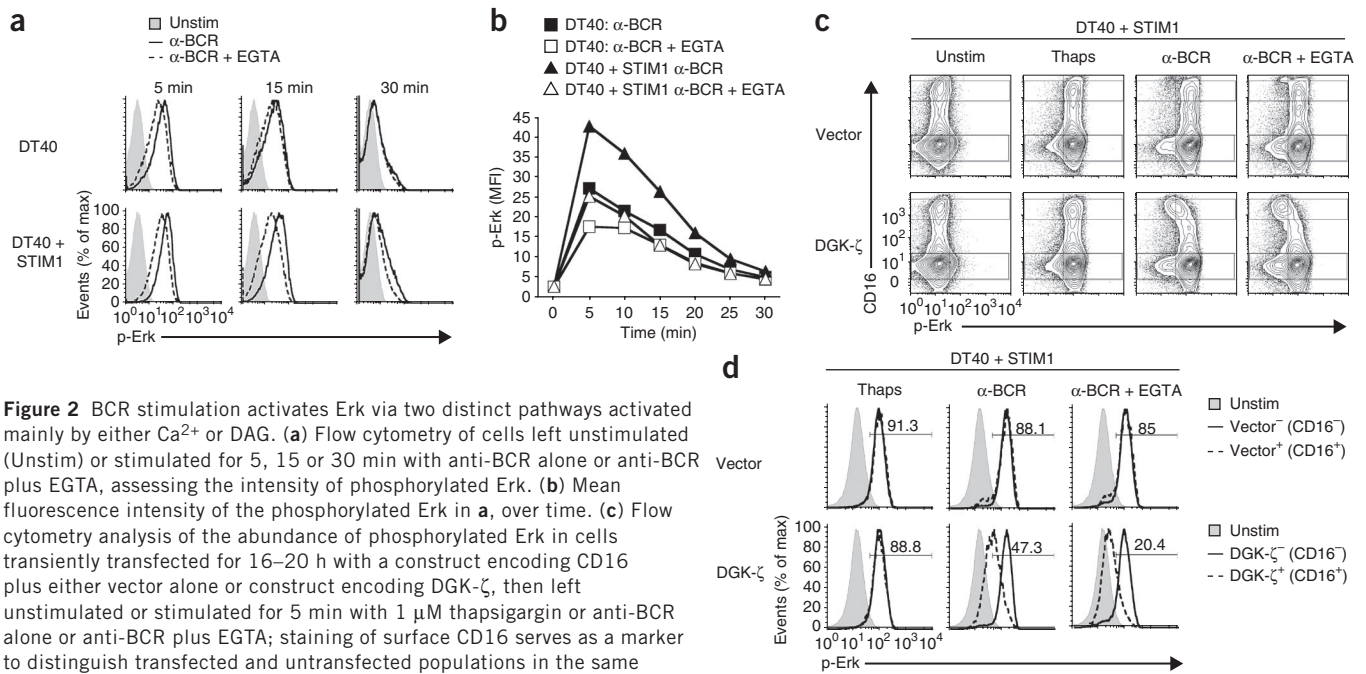


Figure 2 BCR stimulation activates Erk via two distinct pathways activated mainly by either Ca^{2+} or DAG. **(a)** Flow cytometry of cells left unstimulated (Unstim) or stimulated for 5, 15 or 30 min with anti-BCR alone or anti-BCR plus EGTA, assessing the intensity of phosphorylated Erk. **(b)** Mean fluorescence intensity of the phosphorylated Erk in **a**, over time. **(c)** Flow cytometry analysis of the abundance of phosphorylated Erk in cells transiently transfected for 16–20 h with a construct encoding CD16 plus either vector alone or construct encoding DGK- ζ , then left unstimulated or stimulated for 5 min with 1 μM thapsigargin or anti-BCR alone or anti-BCR plus EGTA; staining of surface CD16 serves as a marker to distinguish transfected and untransfected populations in the same sample (gated populations in **c**). **(d)** The phosphorylated Erk response in each population in **c**; numbers above bracketed lines indicate percent cells positive for phosphorylated Erk in the corresponding CD16 $^{+}$ population. Data are representative of at least five (**a,b**) or three (**c,d**) independent experiments.

during either stimulation regimen rescued the cells from apoptosis. Therefore, Ca^{2+} -dependent proapoptotic signals are enhanced in DT40 cells overexpressing STIM1.

Greater SOCE leads to Ca^{2+} -dependent Erk activation

We examined the tyrosine-phosphorylation profile of DT40 cells overexpressing STIM1 after stimulation for 2 min or 5 min with thapsigargin and observed robust and sustained tyrosine phosphorylation of a band of about 42 kilodaltons that was only modestly detectable in thapsigargin-stimulated wild-type DT40 cells (**Fig. 1c**). Immunoprecipitation of this protein with antibody to phosphorylated tyrosine (**Fig. 1d**), followed by mass spectrometry, identified this band as Erk2. To confirm the identity of this protein, we stimulated wild-type DT40 cells or DT40 cells overexpressing STIM1 over time with thapsigargin or CPA in the presence or absence of extracellular Ca^{2+} and analyzed the responses of phosphorylated Erk by flow cytometry. Although Ca^{2+} -dependent activation of Erk was modest and short-lived in wild-type DT40 cells, it was robust and sustained in DT40 cells overexpressing STIM1 (**Fig. 1e,f** and **Supplementary Fig. 2b**). Chelation of extracellular Ca^{2+} by EGTA effectively abrogated the thapsigargin- or CPA-induced phosphorylated Erk response, which demonstrated that the robust Erk activation observed in the DT40 cells overexpressing STIM1 was due to the greater SOCE in these cells.

Antigen-induced activation of Erk in lymphocytes is thought to be DAG dependent and mostly Ca^{2+} independent^{23–27}. However, we hypothesized that a parallel, Ca^{2+} -driven pathway to Erk may become relevant in B cells when SOCE is more intense than the limited DAG signals¹⁰ and longer lasting than the DAG signal. DT40 cells overexpressing STIM1 had greater and more prolonged production of phosphorylated Erk in response to BCR stimulation than did wild-type DT40 cells, and the greater amplitude and duration of the response depended on extracellular Ca^{2+} (**Fig. 2a,b**). To determine whether this pathway to Erk was triggered mainly by Ca^{2+} and

less by DAG, we used diacylglycerol kinase- ζ (DGK- ζ), which converts DAG to phosphatidic acid, thereby inhibiting DAG-dependent responses²⁸. We transfected DT40 cells overexpressing STIM1 with plasmid expressing DGK- ζ and also with plasmid expressing CD16 as a surrogate cell surface marker for transfection. We then stimulated the cells with either thapsigargin or a dose of antibody to BCR (anti-BCR) that elicited a phosphorylated Erk response equivalent to that of the untransfected population (**Fig. 2c,d**). DGK- ζ expression did not inhibit thapsigargin-induced Ca^{2+} -dependent phosphorylation of Erk (**Fig. 2c,d**). In contrast, BCR crosslinking, which triggers DAG production as well as SOCE, elicited a phosphorylated Erk response that was partially inhibited by DGK- ζ . The addition of EGTA at the time of BCR crosslinking led to further inhibition of the phosphorylated Erk response, which demonstrated that simultaneous inhibition of Ca^{2+} and DAG almost entirely ablated Erk activation in these cells. Thus, BCR stimulation can activate Erk via distinct DAG- or Ca^{2+} -dependent pathways, and the kinetics of Ca^{2+} entry and DAG production affect the relative contributions of these pathways to the overall response.

Ca^{2+} -Erk signaling in bone marrow developing B cells

We next investigated whether the activation of the Ca^{2+} -Erk pathway that we observed in our DT40 B cell model with STIM1 expression also occurred in primary B cells. We stimulated bone marrow cells from wild-type C57BL/6 mice with thapsigargin over time, then fixed the cells and made them permeable, and stained them for phosphorylated Erk in combination with cell surface markers, followed by flow cytometry. Only immature and transitional B cells showed robust Ca^{2+} -dependent Erk activation; earlier precursors or mature recirculating B cells did not (**Fig. 3**). Ca^{2+} -dependent Erk activation was less robust in splenic transitional subsets than in bone marrow immature and transitional cells (data not shown), which suggested that this pathway is more relevant in the bone marrow. Thus, B cells are altered developmentally to allow the activation of this pathway

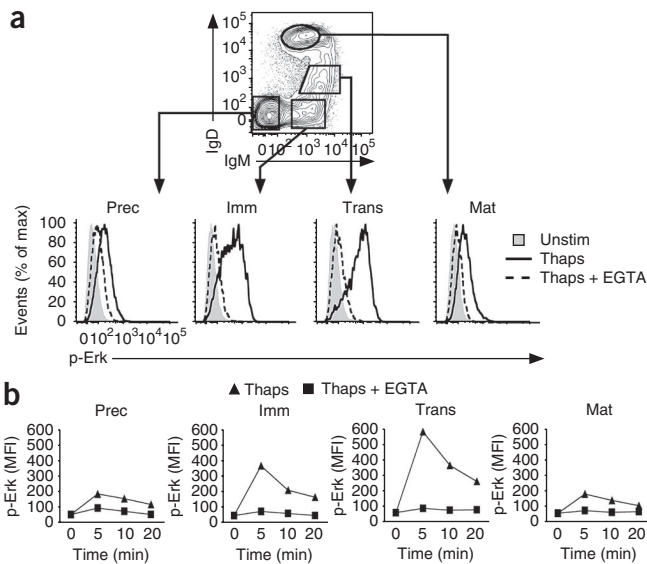


Figure 3 Ca^{2+} -dependent Erk activation occurs selectively at stages of negative selection in primary bone marrow B cells. **(a)** Flow cytometry of wild-type C57BL/6 bone marrow cells stimulated with thapsigargin, then fixed and made permeable and stained for phosphorylated Erk along with cell surface markers; B220^+ cells were gated (top) in four subsets defined as $\text{B220}^+\text{IgM}^-\text{IgD}^-$ (precursors (Prec)), $\text{B220}^+\text{IgM}^+\text{IgD}^-$ (immature (Imm)), $\text{B220}^+\text{IgM}^{\text{hi}}\text{IgD}^{\text{int}}$ (transitional (Trans)) and $\text{B220}^+\text{IgM}^{\text{lo}}\text{IgD}^+$ (mature recirculating (Mat)). Below, the phosphorylated Erk response of each subset. **(b)** Mean fluorescence intensity of the phosphorylated Erk response for each subset in **a** over time. Data are representative of at least three experiments.

specifically in bone marrow B cell populations known to be highly sensitive to apoptosis, during which an important checkpoint for the deletion of self-reactive B cells occurs.

Loss of developing B cells overexpressing STIM1

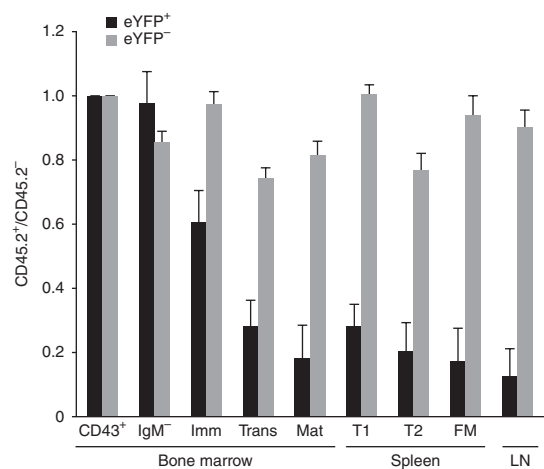
We next hypothesized that, similar to the effect observed in DT40 cells, increasing STIM1 in bone marrow hematopoietic progenitors might increase SOCE, enhance Ca^{2+} -dependent Erk signaling and sensitize developing B cells to negative selection. To test our hypothesis, we infected bone marrow hematopoietic stem cells expressing different congenic markers with retrovirus carrying eYFP or eYFP-STIM1. We used these cells in competitive repopulation experiments and monitored the survival of eYFP-STIM1⁺ B cells throughout development relative to that of eYFP⁺ B cells. We found that eYFP-STIM1⁺ cells were outcompeted by eYFP⁺ cells (Fig. 4), which resulted in very low numbers of eYFP-STIM1⁺ peripheral B cells. The greatest loss of STIM1⁺ B cells occurred in bone marrow stages that correlated with the developmental onset of Ca^{2+} -dependent Erk activation. Thus, increasing STIM1 expression conferred a competitive disadvantage to developing B cells at the same stages that are most sensitive to thapsigargin-induced activation of Erk in unmanipulated bone marrow B lineage cells. To test whether this outcompetition was due to more negative selection, we examined the effect of STIM1 on developing MD4-transgenic B cells, which express a transgenic BCR that recognizes hen egg lysozyme (HEL). We infected hematopoietic stem

Figure 4 STIM1 overexpression confers a competitive disadvantage to developing B cells. Flow cytometry of bone marrow, splenic and lymph node (LN) cells from the lethally irradiated $\text{CD45.2}^+\text{CD45.2}^+$ recipients ($n = 5$) of $\text{CD45.1}^+\text{CD45.1}^+$ or $\text{CD45.1}^+\text{CD45.2}^+$ purified bone marrow hematopoietic stem cells infected with retrovirus encoding eYFP or eYFP-STIM1, respectively, mixed at a ratio of 1:1 and injected into hosts along with uninfected carrier bone marrow of the same genotype, analyzed 8–10 weeks after injection after staining for cell surface markers. Results are presented as the ratio of $\text{CD45.1}^+\text{CD45.2}^+$ cells to $\text{CD45.1}^+\text{CD45.1}^+$ cells for the infected (eYFP⁺) or uninfected (eYFP⁻) populations at various stages in B cell development (corresponding to the ratio of eYFP-STIM1⁺ to eYFP⁺ in the infected population): bone marrow B cell subsets as defined **Figure 3**; splenic B cell subsets defined as $\text{B220}^+\text{CD21}^-\text{CD23}^-$ (transitional 1 (T1)), $\text{B220}^+\text{IgM}^{\text{hi}}\text{IgD}^{\text{hi}}$ (transitional 2 (T2)), $\text{B220}^+\text{IgM}^{\text{lo}}\text{IgD}^{\text{hi}}$ (follicular mature (FM)). Data are from one experiment representative of at least three independent experiments (error bars, s.e.m.).

cells from MD4 mice with eYFP-STIM1 and injected the cells into lethally irradiated wild-type recipient mice. We monitored the survival of MD4 B cells transduced with eYFP-STIM1 relative to that of nontransduced MD4 B cells throughout development. In the absence of antigen, MD4 B cells overexpressing eYFP-STIM1 competed efficiently with nontransduced cells during bone marrow development (**Supplementary Fig. 3**). In fact, mice occasionally demonstrated greater population expansion of eYFP-STIM1⁺ cells relative to that of nontransduced cells, an effect opposite to that observed in mice with an unrestricted B cell repertoire. Therefore, restricting the BCR repertoire to a transgenic HEL-specific BCR in the absence of antigen (HEL) was sufficient to correct the competitive disadvantage of STIM1-overexpressing B cells. These findings demonstrate that STIM1 sensitizes developing B cells to negative selection.

RasGRP-dependent Ca^{2+} -Erk signaling is proapoptotic

We next investigated the mechanism by which SOCE activates Erk to determine if a causal relationship exists between this pathway and apoptosis. Calcium increases are not generally thought to modulate the mitogen-activated protein kinase pathways leading to Erk activation. RasGRP and SOS are guanine nucleotide-exchange factors for the GTPase Ras involved in the production of RasGTP upstream of Erk activation in lymphocytes^{25,29–33}. RasGRP proteins contain both DAG-binding C1 domains and Ca^{2+} -binding EF hands, and they have been proposed to mediate proapoptotic signals in B cells^{34,35}. Although DAG is important for RasGRP activity, we hypothesized that under conditions of considerable SOCE, Ca^{2+} could potentially trigger activation of RasGRP as well, leading to Erk activation. We first transiently transfected *Rasgrp1*^{-/-}*Rasgrp3*^{-/-} or *Sos1*^{-/-}*Sos2*^{-/-} DT40 cells³² with eYFP-STIM1 and assessed the ability of these cells to support Erk activation in response to thapsigargin. Thapsigargin-induced activation of Erk was almost entirely abrogated in RasGRP-deficient cells overexpressing STIM1 but was completely unaffected in



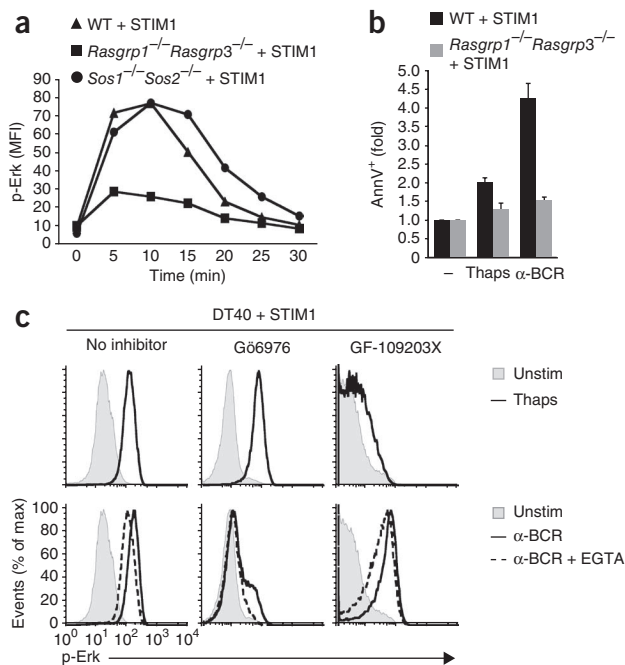


Figure 5 Activation of Erk downstream of Ca^{2+} requires RasGRP.

(a) Intensity of phosphorylated Erk in the eYFP-STIM1⁺ population of wild-type (WT), *Rasgrp1*^{-/-}*Rasgrp3*^{-/-} or *Sos1*^{-/-}*Sos2*^{-/-} DT40 cells transiently transfected with the eYFP-STIM1 retrovirus, then stimulated with thapsigargin, fixed and made permeable and stained for phosphorylated Erk. (b) Annexin V on the surface of cells stably overexpressing STIM1, left unstimulated or stimulated for 8 h with thapsigargin or anti-BCR, presented relative to that on unstimulated cells. (c) Intensity of phosphorylated Erk in wild-type DT40 cells stably overexpressing STIM1, left untreated (No inhibitor) or treated for 5 min with the PKC inhibitor Gö6976 or GF-109203X, then left unstimulated or stimulated for 5 min with thapsigargin (top row) or anti-BCR alone or with EGTA (bottom row). Data are representative of two independent experiments (a), five experiments (b; error bars, s.e.m.) or at least two independent experiments (c).

SOS-deficient cells overexpressing STIM1 (Fig. 5a). We thus generated *Rasgrp1*^{-/-}*Rasgrp3*^{-/-} DT40 cell lines stably overexpressing eYFP-STIM1 (Supplementary Fig. 4a), which had more SOCE, similar to that in wild-type DT40 cells overexpressing STIM1 (Supplementary Fig. 4b). As expected, given the results of the transient transfection experiments, these cells showed a nearly complete loss of Erk activation in response to thapsigargin (Supplementary Fig. 4c). Deficiency in RasGRP rescued DT40 cells from BCR-induced apoptosis, even when STIM1 was overexpressed (Fig. 5b). These results demonstrate that RasGRP is needed to mediate Erk activation by Ca^{2+} and disrupting Ca^{2+} -dependent activation of RasGRP and Erk is sufficient to inhibit antigen receptor-induced apoptosis.

PKC-mediated phosphorylation of RasGRP is known to be important for its activation^{25,26,36,37}. To determine whether Ca^{2+} -dependent activation of Erk requires PKC activity, we examined the effect of two different PKC inhibitors, GF-109203X and Gö6976, on thapsigargin- or anti-BCR-induced phosphorylation of Erk. Unexpectedly, the two PKC inhibitors had opposite effects. GF-109203X potently inhibited the response to thapsigargin while having a minor effect on the anti-BCR response. Gö6976 did not inhibit the response to thapsigargin but inhibited most of the anti-BCR-induced phosphorylated Erk response, with the remaining phosphorylated Erk being Ca^{2+} dependent (Fig. 5c). This result was consistent with published studies examining the role of Gö6976 in BCR-induced phosphorylated Erk^{36,37}. Therefore, Gö6976 inhibits the DAG-dependent component of the BCR-mediated Erk response but not the Ca^{2+} -dependent response. In contrast, GF-109203X inhibits the Ca^{2+} -dependent Erk response but not the DAG-dependent response. Although both of these inhibitors are known to inhibit classical PKC proteins with similar potency, their ability to inhibit nonclassical PKC proteins is different. GF-109203X can efficiently block PKC- δ activity, but Gö6976 cannot³⁸, which suggests that this PKC isoform has a critical role in Ca^{2+} -dependent Erk signaling.

Ca^{2+} -Erk signaling requires phosphorylated Ser332 of RasGRP1

The cooperation between PKC and RasGRP proteins has been well documented, but the only phosphorylation site thus far identified as a target of PKC proteins is RasGRP1 Thr184, which corresponds to

Thr133 of RasGRP3 (refs. 36,37). Notably, neither of these sites fits a PKC- δ consensus target sequence. Moreover, phosphorylation of these sites is blocked by Gö6976, which does not inhibit PKC- δ - or Ca^{2+} -dependent Erk activation. Indeed, we found that RasGRP3 Thr133 was not phosphorylated in response to thapsigargin, and a mutant RasGRP1 with replacement of the threonine at position 184 with alanine was largely functional in mediating Erk activation in response to SOCE (data not shown). Therefore, we hypothesized that PKC- δ could potentially phosphorylate RasGRP on other sites and thereby induce activation of a functionally distinct Erk pathway. To test our hypothesis, we selected candidate sites on human RasGRP1 on the basis of the following three criteria: first, putative sites must have a PKC- δ consensus target sequence (S/TXXR/K, where 'S/T' indicates serine or threonine, 'X' indicates any amino acid, and 'R/K' indicates arginine or lysine); next, these sites should have a predictive phosphorylation score above 0.8 on the Netphos 2.0 server (Center For Biological Sequence Analysis, Technical University of Denmark), which provides predictions for serine-, threonine- and tyrosine-phosphorylation sites in eukaryotic proteins³⁹; and finally, sites should be conserved across species (chicken, mouse and human; Supplementary Fig. 5a). We identified five potential serine or threonine sites on RasGRP1 and individually substituted these with alanine. We transiently transfected RasGRP-deficient DT40 cells overexpressing STIM1 with constructs for these mutants or wild-type human RasGRP1. We then stimulated the transfected cells with thapsigargin and assessed the phosphorylated Erk response in the transfected populations. Four of the five mutant proteins were able to support Ca^{2+} -dependent Erk activation (Supplementary Fig. 5b). However, the mutant RasGRP1 with substitution of alanine for serine at position 332 (RasGRP1(S332A)) was completely deficient in activation of this pathway, which resulted in activation of Erk similar to that in the parental RasGRP-deficient cells (Fig. 6a). Cells transfected with the RasGRP1(S332A) construct expressed the mutant RasGRP1 protein in an amount similar to that observed for wild-type RasGRP1 protein in cells transfected with the wild-type RasGRP1 construct (Supplementary Fig. 6), which indicated that this effect was not due to lack of expression or lower stability of the mutant protein. We then assessed the ability of this mutant to support DAG-mediated activation of Erk. Notably, in cells stimulated with anti-BCR in the presence of EGTA, S332A RasGRP1 was able to support Erk activation, albeit less than wild-type RasGRP1 was (Fig. 6b). This result demonstrated that the S332A substitution did not result in a completely inactive nucleotide-exchange factor but instead that Ser332 is a crucial site that modulates the selective responsiveness of the exchange factor to Ca^{2+} -induced signals. To further address whether phosphorylation of Ser332 is involved in Ca^{2+} -induced Erk activation, we generated a phosphomimetic RasGRP1 mutant with substitution of aspartic acid for serine at position 332. This mutant

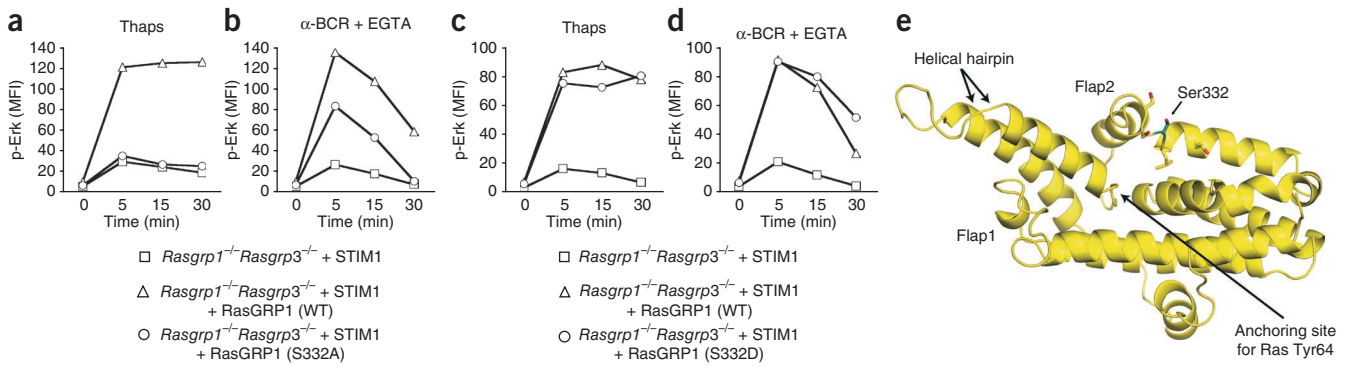


Figure 6 Phosphorylation of RasGRP1 at Ser332 is required for the restoration of Ca^{2+} -dependent Erk activation by RasGRP1 in RasGRP-deficient cells. (a,b) Intensity of the phosphorylated Erk response over time in RasGRP-deficient cells overexpressing STIM1, transiently transfected with constructs encoding wild-type or S332A Myc-tagged human RasGRP1, then stimulated with thapsigargin (a) or with anti-BCR plus EGTA (b). (c,d) Analysis of the phosphorylated Erk response as in a, but in cells transfected with constructs encoding wild-type RasGRP1 or mutant RasGRP1 with substitution of aspartic acid for serine at position 332 (S332D), then stimulated with thapsigargin (c) or anti-BCR plus EGTA (d). (e) Three-dimensional homology model of the structure of the CDC25 domain of mouse RasGRP1 made with the RasGRF1 CDC25 domain as a template, showing the potential phosphorylation site at Ser332 (blue sticks) in flap2 abutting the helical hairpin; stick-and-ball indicates residues within 3.2 Å of Ser332. Data are representative of at least four independent experiments (a,b) or two independent experiments (c,d).

was fully functional and induced Erk activation in response to Ca^{2+} to the same extent that wild-type RasGRP1 did (Fig. 6c). The same was true of the DAG-dependent BCR response, as measured by stimulation with anti-BCR in the presence of EGTA (Fig. 6d). These results demonstrate that phosphorylation of Ser332 is absolutely required for Ca^{2+} -dependent BCR-induced Erk activation but not for the DAG-dependent BCR-induced Erk activation. Notably, unstimulated cells expressing the phosphomimetic mutant RasGRP1 did not show constitutive Erk activation, which suggested that although phosphorylation of Ser332 is required, it may not be sufficient to constitutively activate the pathway. Given the robust effect of the S332A substitution on the ability of RasGRP1 to mediate Ca^{2+} -dependent Erk activation, we

did homology modeling with the ModWeb server⁴⁰ and the template mouse RasGRF1 (Protein Data Bank accession code, 2IJE)⁴¹ to gain insight into the possible role this site might have in the regulation of RasGRP1 activity (Fig. 6e). Notably, this model predicted that Ser332 is in the flap2 region of the Ras-interacting CDC25 domain, where a phosphorylation event could affect the binding of Ras and/or the positioning of the catalytic helical hairpin.

Developmental regulation of STIM1, RasGRP and PKC- δ

To determine whether developmental regulation of protein expression might have a role in the selective activation of this pathway during negative selection, we sorted bone marrow

B cell subsets and examined the expression of STIM1, PKC- δ and RasGRP proteins. Consistent with the proposal of a role for this pathway in antigen-induced apoptosis, expression of RasGRP1, RasGRP3, PKC- δ and STIM1 was higher at the bone marrow transitional stage, at which negative selection occurs (Supplementary Fig. 7), than in earlier B cell subsets. This stage was also the point at which thapsigargin-induced SOCE with greater amplitude and faster kinetics (Supplementary Fig. 8) and maximal thapsigargin-induced phosphorylated Erk responses (Fig. 3) occurred. Expression of RasGRP1, PKC- δ and STIM1 was then downregulated in mature B cells, whereas RasGRP3 abundance increased further in mature B cells. The pattern of PKC- δ expression was consistent with published results examining expression of *lacZ* introduced into the *Prkcd* locus in the *Prkcd*^{-/-} mice²¹. Likewise, the greater abundance RasGRP1 and PKC- δ protein in bone marrow transitional B cells was also consistent with robust changes in mRNA abundance reported on the Immunological Genome Research Project website. These results suggest that transient increases in RasGRP1, PKC- δ and

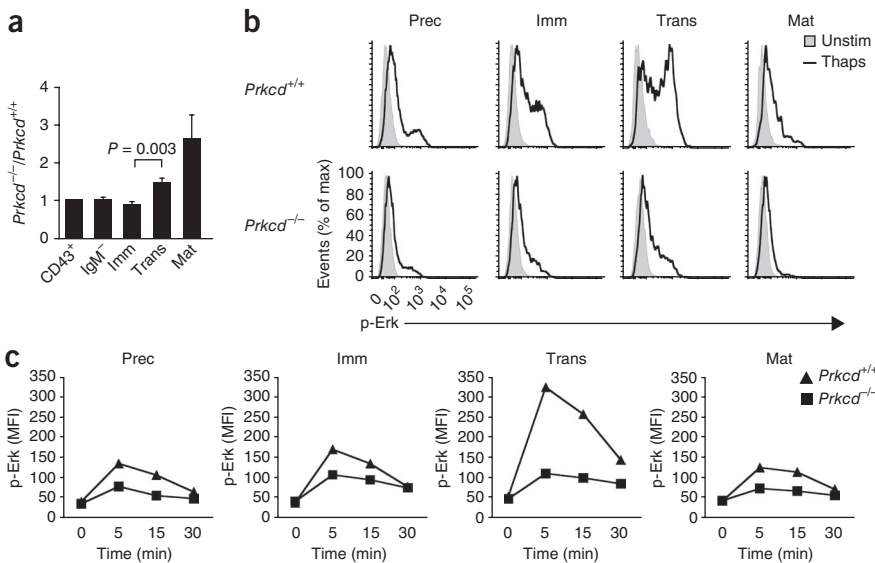


Figure 7 PKC- δ is required for Ca^{2+} -dependent activation of Erk in developing bone marrow cells. (a) Ratio of *Prkcd*^{-/-} cells to wild-type (*Prkcd*^{+/+}) cells throughout B cell development in lethally irradiated recipients ($n = 8$) of *Prkcd*^{-/-} and wild-type bone marrow cells (bearing different CD45 congenic markers) mixed at a ratio of 1:1, analyzed 6–8 weeks after injection. P value, paired t -test. (b) The phosphorylated Erk response in *Prkcd*^{-/-} and wild-type bone marrow cells left unstimulated or stimulated with thapsigargin, analyzed by flow cytometry. (c) Intensity of the phosphorylated Erk in b, presented relative to that in resting cells. Data are from one experiment representative of two independent experiments (a; error bars, s.e.m.) or at least four independent experiments (b,c).

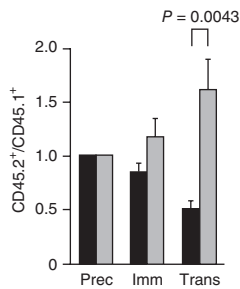


Figure 8 PKC- δ is required for STIM1-mediated sensitization of bone marrow B cells to negative selection. Flow cytometry of cells from lethally irradiated CD45.1⁺CD45.2⁺ heterozygous recipients reconstituted with CD45.1⁺CD45.1⁺ hematopoietic stem cells infected with eYFP-expressing retrovirus and mixed at a ratio of 1:1 with wild-type (black bars; $n = 8$ recipients) or *Prkcd*^{-/-} (gray bars; $n = 11$ recipients) CD45.2⁺CD45.2⁺ hematopoietic stem cells infected with the eYFP-STIM1 retrovirus, then injected into hosts along with uninfected carrier bone marrow of the same genotype, followed by analysis 8–10 weeks after injection (as in Fig. 4). P value, unpaired t -test. Data are from one experiment representative of three independent experiments (error bars, s.e.m.).

STIM1 could contribute to the ‘preferential’ activation of the Ca²⁺-Erk pathway in developing B cells, and that downregulation of these proteins in mature B cells may contribute to the loss of sensitivity to antigen-induced apoptosis. In contrast, the expression pattern of RasGRP3 suggests this protein may also be involved in DAG-mediated Erk signaling in mature B cells.

Ca²⁺-Erk signaling in developing B cells requires PKC- δ

The idea that PKC- δ may be required for Ca²⁺-dependent Erk activation during B cell negative selection is notable, given the phenotype of *Prkcd*^{-/-} mice^{21,22}. These mice have twofold and sevenfold more B cells in the spleen and lymph nodes, respectively. In these mice, self-reactive B cells develop and terminally differentiate but fail to undergo anergy. *Prkcd*^{-/-} mice develop antinuclear antibodies and die prematurely at 9–12 months of age because of autoimmune disease. Published studies of these mice have focused on defects in peripheral B cell homeostasis that contribute to the phenotype⁴². However, given the developmental regulation of Ca²⁺-dependent Erk activation, we hypothesized that the phenotype of the *Prkcd*^{-/-} mice may be at least partly due to an inability to activate the Ca²⁺-regulated Erk pathway during B cell negative selection. We did competitive-repopulation experiments in which we mixed *Prkcd*^{-/-} and wild-type bone marrow cells at a ratio of 1:1 and injected the mixture into lethally irradiated mice. As expected, the *Prkcd*^{-/-} B cells outcompeted the wild-type cells (Fig. 7a). Notably, the earliest developmental stage at which we observed this effect coincided with the bone marrow stage at which Ca²⁺-dependent Erk activation occurred and at which higher STIM1 expression enhanced negative selection, whereas we did not observe it in the developmental stages before antigen receptor expression. This observation suggests that the competitive advantage of *Prkcd*^{-/-} B cells relates to an alteration of developmental stage-specific signals.

We then hypothesized that the competitive advantage of *Prkcd*^{-/-} bone marrow transitional B cells might relate to a loss of proapoptotic Ca²⁺-Erk signaling at this developmental stage. Thapsigargin-induced SOCE in *Prkcd*^{-/-} cells was similar to or slightly greater than that in wild-type cells (Supplementary Fig. 8). However, Ca²⁺-dependent Erk activation was markedly impaired in developing *Prkcd*^{-/-} bone marrow B cells (Fig. 7b,c). The cell populations analyzed contain similar

numbers of newly generated B cells in both genotypes, as shown by the rate of incorporation of the thymidine analog BrdU (Supplementary Fig. 9). Therefore, loss of Ca²⁺-dependent Erk signaling in transitional *Prkcd*^{-/-} bone marrow B cells may have enhanced the survival of self-reactive B cells that would otherwise undergo apoptosis, thus setting the stage for the previously described autoimmune phenotype (Supplementary Fig. 10a,b). In contrast, enhancing the activation of this pathway by increasing the concentration of STIM1 (Fig. 4) may have led to more activation of this pathway, resulting in more negative selection (Supplementary Fig. 10c).

PKC- δ deficiency rescues STIM1-overexpressing B cells

Finally, we sought to determine whether the STIM1-mediated sensitization of B cells to negative selection in the bone marrow (Fig. 4) depended on this SOCE–PKC- δ –RasGRP–Erk pathway. We infected wild-type and *Prkcd*^{-/-} hematopoietic stem cells with the eYFP-STIM1 retrovirus, then mixed those cells at a ratio 1:1 with wild-type cells infected with the eYFP retrovirus and injected the mixed population into lethally irradiated recipient mice. We analyzed the recipients 6–8 weeks after injection and determined the ratio of eYFP-STIM1⁺ cells to eYFP⁺ cells throughout the bone marrow developing B cell populations. As shown above (Fig. 4), wild-type B cells overexpressing STIM1 were at a competitive disadvantage at the immature and transitional stages in the bone marrow (Fig. 8). In contrast, *Prkcd*^{-/-} B cells overexpressing STIM1 had a competitive advantage over wild-type cells expressing eYFP alone (Fig. 8), which indicated that PKC- δ is needed for STIM1 to sensitize B cells to negative selection at this developmental stage. Notably, the composition of the mature recirculating B cell population in these mice was highly variable (data not shown), perhaps indicative of a more complex epistatic relationship between PKC- δ and STIM1 in peripheral B cell homeostasis. Nevertheless, these results further support a model in which Ca²⁺-dependent Erk signaling, mediated by PKC- δ and RasGRP, sets a threshold for negative selection in the bone marrow (Supplementary Fig. 10).

DISCUSSION

Our data have demonstrated the existence of a Ca²⁺-dependent proapoptotic pathway to Erk activation, which mediates a critical checkpoint during B cell development. We therefore propose a model in which Ca²⁺ and DAG direct Erk to distinct functional outcomes during B cell development. Because DAG and inositol-(1,4,5)-trisphosphate are produced at equal molar concentrations downstream of the hydrolysis of phosphatidylinositol-(4,5)-bisphosphate mediated by phospholipase C- γ , DAG production is inextricably linked to SOCE induced by inositol-(1,4,5)-trisphosphate. However, the amplitude and duration of DAG production and SOCE depends mainly on proteins that amplify or negatively regulate these second messengers. For example, more STIM1 (which we observed in bone marrow transitional cells) may contribute to the amplification of SOCE. In contrast, less DAG production, which has been reported in immature B cells¹⁰, may be the result of rapid DAG turnover mediated by DAG kinases, DAG acyltransferases or DAG lipases, all of which metabolize DAG into different products. Data from the Immunological Genome Research Project website show that the abundance of mRNA for some of these proteins, such as DGK- δ , DGK- τ , DGK- η , DGL β or DGAT2L6, changes during B cell development in ways that may affect DAG metabolism. In addition, we have found that considerable changes in the expression of proteins that mediate the activation of Erk pathways during development also contributed to their amplification, as demonstrated by the much higher expression of RasGRP1 and PKC- δ in transitional bone marrow B cells than in other B cell subsets. These changes in expression

are probably critical in setting the appropriate threshold of antigenic signal strength that results in negative selection.

The involvement of PKC- δ in this proapoptotic Erk pathway was not expected. PKC- δ has been linked to the apoptosis of many cell types^{43,44}, but the potential involvement of proapoptotic Ras-Erk signaling as an effector pathway downstream of PKC- δ has not been explored, to our knowledge. Therefore, our data linking PKC- δ to antigen-induced proapoptotic Ras-Erk signaling establish a new paradigm that could be tested in other systems in which PKC- δ is important in mediating apoptosis. *Prkcd*^{-/-} mice have a defect in peripheral B cell homeostasis that increases the lifespan of B cells and is independent of selection events^{21,42}. However, our data showing the involvement of PKC- δ in proapoptotic Erk signaling during negative selection now suggest that loss of PKC- δ may also result in previously unrecognized alterations to the B cell repertoire that contribute to the disease pathology of the mice. Notably, PKC- δ has been reported to be dispensable in a transgenic model of negative selection mediated by the expression of membrane-bound HEL in MD4 mice, which have B cells specific for a transgenic BCR that recognizes HEL²¹; this indicates that this may not be the only pathway that mediates the negative selection of B cells. However, membrane-bound HEL in that model provides an exceedingly strong antigenic stimulus, in particular to a high-affinity BCR transgene, that may override mechanisms that establish selection thresholds for many antigens in normal cells, thus leading to the deletion of B cells at the earliest bone marrow immature stage^{45,46}. Because the onset of PKC- δ -mediated, Ca²⁺-dependent Erk activation occurs in IgM^{hi}IgD^{int} bone marrow transitional B cells, it is not unexpected that the membrane-bound HEL system did not demonstrate the role of PKC- δ in negative selection.

The activation of Ras and Erk has been intensively studied in lymphocytes and has mostly been thought of as DAG dependent and Ca²⁺ independent. Our findings have demonstrated that more than one pathway leads to Erk activation in B lymphocytes, and here we have shown that a Ca²⁺-dependent Erk activation pathway directed the functional outcome of the stimulus toward an apoptotic fate in developing B cells. Because RasGRP1 is prominently and exclusively expressed in B cell subsets in which this pathway is active, we focused our efforts on defining the biochemical mechanisms by which Ca²⁺ may influence its function. We have thus identified RasGRP1 Ser332 as a potential phosphorylation site that is a likely PKC- δ target and that was required for Ca²⁺-dependent Erk activation. Unexpectedly, this site is located in the CDC25 domain of RasGRP1, the domain that actually mediates the interaction with Ras and consequently the nucleotide-exchange function of the protein. Because of this, a phosphorylation event that preserves nucleotide-exchange function (as is the case with Ser332) is unlikely to trigger structural reorganization of the protein. On the basis of homology modeling with the RasGRF1 CDC25 domain^{41,47}, we predict that this site is in the flap2 region of the CDC25 domain, which may have a role in positioning the catalytic helical hairpin of the exchange factor for catalysis. This residue is close to the Ras-binding site, and because of the increase in negative charge associated with phosphorylation, electrostatic interactions may influence which Ras isoform interacts with RasGRP1. This may help explain how distinct Ras protein signaling pathways that rely on Erk achieve specificity.

The Ras-Erk pathway is very promiscuous in terms of potential substrates, and it has been suggested that specificity is achieved through compartmentalization mediated by scaffolds that constrain Erk to signaling complexes, where it can be activated by the appropriate stimuli and simultaneously gain access to appropriate substrates⁴⁸⁻⁵⁰. As mentioned above, phosphorylation of RasGRP1

at Ser332 could potentially contribute to such specificity. However, although it is clear that phosphorylation of RasGRP1 at Ser332 was essential for the induction of activation of this Erk pathway by SOCE, the results obtained with the phosphomimetic mutant suggested that this event was also not sufficient to activate it and that other Ca²⁺-dependent events may be required. Because PKC- δ is not thought to bind Ca²⁺ directly, it is possible that the binding of Ca²⁺ to RasGRP1 via the EF hands contributes to the promotion of RasGRP activity, possibly by facilitating the interaction with PKC- δ . Moreover, at this point we cannot exclude the possibility that other Ca²⁺-responsive proteins may have a role in this signaling complex, perhaps by further modifying PKC- δ and/or RasGRP and potentiating their activity. Concentration gradients of DAG and Ca²⁺ are also known to affect the localization of signaling proteins and may contribute to directing distinct Erk pathways to unique compartments in the cell. Notably, results obtained with thymocytes have indicated the involvement of differences in the localization of mitogen-activated protein kinase signals in setting the thresholds of positive and negative selection⁵¹. Those findings, combined with our data, suggest that Ca²⁺ and DAG may control selection by directing the assembly and localization of different mitogen-activated protein kinase signaling complexes.

METHODS

Methods and any associated references are available in the online version of the paper at <http://www.nature.com/natureimmunology/>.

Note: Supplementary information is available on the Nature Immunology website.

ACKNOWLEDGMENTS

We thank the Sandler-Moore Mass Spectrometry Core Facility at the University of California at San Francisco (funded by the Sandler Family Foundation, the Gordon and Betty Moore Foundation and the National Cancer Institute of the US National Institutes of Health (P30 CA82103)) for assistance in protein identification; the Flow Cytometry Core Facility at the Department of Pathology and Diabetes Center of the University of California at San Francisco for assistance; G. Koretzky (University of Pennsylvania) for the pEF-Flag-hDGK- ζ plasmid; A. Roque for assistance with animal husbandry; H. Phee and M. Hermiston for critical reading of the manuscript and suggestions; B. Au-Yeung and H. Wang for help with tail-vein injections; and members of the Weiss laboratory for discussions. Supported by the Howard Hughes Medical Institute and the Sidney Kimmel Foundation (J.P.R.).

AUTHOR CONTRIBUTIONS

A.L. designed and did experiments, analyzed the data and wrote the manuscript; P.D. collaborated with A.L. in determining expression of various proteins on sorted bone marrow B cell populations and in collecting reconstituted mice; T.S.F. did homology modeling of RasGRP1; J.L. and T.K. provided reagents; M.L. generated the *Prkcd*^{-/-} mice; J.P.R. designed experiments and provided reagents; and A.W. designed experiments, supervised the research, revised the manuscript and provided support.

COMPETING FINANCIAL INTERESTS

The authors declare no competing financial interests.

Published online at <http://www.nature.com/natureimmunology/>.

Reprints and permissions information is available online at <http://npg.nature.com/reprintsandpermissions/>.

- Gay, D., Saunders, T., Camper, S. & Weigert, M. Receptor editing: an approach by autoreactive B cells to escape tolerance. *J. Exp. Med.* **177**, 999–1008 (1993).
- Goodnow, C.C. *et al.* Altered immunoglobulin expression and functional silencing of self-reactive B lymphocytes in transgenic mice. *Nature* **334**, 676–682 (1988).
- Nemazee, D.A. & Burki, K. Clonal deletion of B lymphocytes in a transgenic mouse bearing anti-MHC class I antibody genes. *Nature* **337**, 562–566 (1989).
- Tiegs, S.L., Russell, D.M. & Nemazee, D. Receptor editing in self-reactive bone marrow B cells. *J. Exp. Med.* **177**, 1009–1020 (1993).
- Wardemann, H. *et al.* Predominant autoantibody production by early human B cell precursors. *Science* **301**, 1374–1377 (2003).

6. Hertz, M. & Nemazee, D. BCR ligation induces receptor editing in IgM⁺IgD⁻ bone marrow B cells in vitro. *Immunity* **6**, 429–436 (1997).
7. Melamed, D., Benschop, R.J., Cambier, J.C. & Nemazee, D. Developmental regulation of B lymphocyte immune tolerance compartmentalizes clonal selection from receptor selection. *Cell* **92**, 173–182 (1998).
8. Benschop, R.J., Brandl, E., Chan, A.C. & Cambier, J.C. Unique signaling properties of B cell antigen receptor in mature and immature B cells: implications for tolerance and activation. *J. Immunol.* **167**, 4172–4179 (2001).
9. Gross, A.J., Lyandres, J.R., Panigrahi, A.K., Prak, E.T. & DeFranco, A.L. Developmental acquisition of the Lyn-CD22-SHP-1 inhibitory pathway promotes B cell tolerance. *J. Immunol.* **182**, 5382–5392 (2009).
10. Hoek, K.L. *et al.* Transitional B cell fate is associated with developmental stage-specific regulation of diacylglycerol and calcium signaling upon B cell receptor engagement. *J. Immunol.* **177**, 5405–5413 (2006).
11. King, L.B., Norvell, A. & Monroe, J.G. Antigen receptor-induced signal transduction imbalances associated with the negative selection of immature B cells. *J. Immunol.* **162**, 2655–2662 (1999).
12. Parekh, A.B. & Putney, J.W. Jr. Store-operated calcium channels. *Physiol. Rev.* **85**, 757–810 (2005).
13. Liou, J. *et al.* STIM is a Ca²⁺ sensor essential for Ca²⁺-store-depletion-triggered Ca²⁺ influx. *Curr. Biol.* **15**, 1235–1241 (2005).
14. Roos, J. *et al.* STIM1, an essential and conserved component of store-operated Ca²⁺ channel function. *J. Cell Biol.* **169**, 435–445 (2005).
15. Zhang, S.L. *et al.* STIM1 is a Ca²⁺ sensor that activates CRAC channels and migrates from the Ca²⁺ store to the plasma membrane. *Nature* **437**, 902–905 (2005).
16. Liou, J., Fivaz, M., Inoue, T. & Meyer, T. Live-cell imaging reveals sequential oligomerization and local plasma membrane targeting of stromal interaction molecule 1 after Ca²⁺ store depletion. *Proc. Natl. Acad. Sci. USA* **104**, 9301–9306 (2007).
17. Luik, R.M., Wu, M.M., Buchanan, J. & Lewis, R.S. The elementary unit of store-operated Ca²⁺ entry: local activation of CRAC channels by STIM1 at ER-plasma membrane junctions. *J. Cell Biol.* **174**, 815–825 (2006).
18. Park, C.Y. *et al.* STIM1 clusters and activates CRAC channels via direct binding of a cytosolic domain to Orai1. *Cell* **136**, 876–890 (2009).
19. Spassova, M.A. *et al.* STIM1 has a plasma membrane role in the activation of store-operated Ca²⁺ channels. *Proc. Natl. Acad. Sci. USA* **103**, 4040–4045 (2006).
20. Wu, M.M., Buchanan, J., Luik, R.M. & Lewis, R.S. Ca²⁺ store depletion causes STIM1 to accumulate in ER regions closely associated with the plasma membrane. *J. Cell Biol.* **174**, 803–813 (2006).
21. Mecklenbrauker, I., Saijo, K., Zheng, N.Y., Leitges, M. & Tarakhovskiy, A. Protein kinase C δ controls self-antigen-induced B-cell tolerance. *Nature* **416**, 860–865 (2002).
22. Miyamoto, A. *et al.* Increased proliferation of B cells and auto-immunity in mice lacking protein kinase C δ . *Nature* **416**, 865–869 (2002).
23. Dower, N.A. *et al.* RasGRP is essential for mouse thymocyte differentiation and TCR signaling. *Nat. Immunol.* **1**, 317–321 (2000).
24. Roose, J. & Weiss, A. T cells: getting a GRP on Ras. *Nat. Immunol.* **1**, 275–276 (2000).
25. Roose, J.P., Mollenauer, M., Gupta, V.A., Stone, J. & Weiss, A. A diacylglycerol-protein kinase C-RasGRP1 pathway directs Ras activation upon antigen receptor stimulation of T cells. *Mol. Cell Biol.* **25**, 4426–4441 (2005).
26. Teixeira, C., Stang, S.L., Zheng, Y., Beswick, N.S. & Stone, J.C. Integration of DAG signaling systems mediated by PKC-dependent phosphorylation of RasGRP3. *Blood* **102**, 1414–1420 (2003).
27. Downward, J., Graves, J.D., Warne, P.H., Rayter, S. & Cantrell, D.A. Stimulation of p21ras upon T-cell activation. *Nature* **346**, 719–723 (1990).
28. Zhong, X.P. *et al.* Enhanced T cell responses due to diacylglycerol kinase zeta deficiency. *Nat. Immunol.* **4**, 882–890 (2003).
29. Das, J. *et al.* Digital signaling and hysteresis characterize ras activation in lymphoid cells. *Cell* **136**, 337–351 (2009).
30. Ebinu, J.O. *et al.* RasGRP, a Ras guanyl nucleotide-releasing protein with calcium- and diacylglycerol-binding motifs. *Science* **280**, 1082–1086 (1998).
31. Ebinu, J.O. *et al.* RasGRP links T-cell receptor signaling to Ras. *Blood* **95**, 3199–3203 (2000).
32. Oh-hora, M., Johmura, S., Hashimoto, A., Hikida, M. & Kurosaki, T. Requirement for Ras guanine nucleotide releasing protein 3 in coupling phospholipase C- γ 2 to Ras in B cell receptor signaling. *J. Exp. Med.* **198**, 1841–1851 (2003).
33. Roose, J.P., Mollenauer, M., Ho, M., Kurosaki, T. & Weiss, A. Unusual interplay of two types of Ras activators, RasGRP and SOS, establishes sensitive and robust Ras activation in lymphocytes. *Mol. Cell Biol.* **27**, 2732–2745 (2007).
34. Guilbault, B. & Kay, R.J. RasGRP1 sensitizes an immature B cell line to antigen receptor-induced apoptosis. *J. Biol. Chem.* **279**, 19523–19530 (2004).
35. Stang, S.L. *et al.* A proapoptotic signaling pathway involving RasGRP, Erk, and Bim in B cells. *Exp. Hematol.* **37**, 122–134 (2009).
36. Aiba, Y. *et al.* Activation of RasGRP3 by phosphorylation of Thr-133 is required for B cell receptor-mediated Ras activation. *Proc. Natl. Acad. Sci. USA* **101**, 16612–16617 (2004).
37. Zheng, Y. *et al.* Phosphorylation of RasGRP3 on threonine 133 provides a mechanistic link between PKC and Ras signaling systems in B cells. *Blood* **105**, 3648–3654 (2005).
38. Martiny-Baron, G. *et al.* Selective inhibition of protein kinase C isozymes by the indolocarbazole Go 6976. *J. Biol. Chem.* **268**, 9194–9197 (1993).
39. Blom, N., Gammeltoft, S. & Brunak, S. Sequence and structure-based prediction of eukaryotic protein phosphorylation sites. *J. Mol. Biol.* **294**, 1351–1362 (1999).
40. Eswar, N. *et al.* Tools for comparative protein structure modeling and analysis. *Nucleic Acids Res.* **31**, 3375–3380 (2003).
41. Freedman, T.S. *et al.* A Ras-induced conformational switch in the Ras activator Son of sevenless. *Proc. Natl. Acad. Sci. USA* **103**, 16692–16697 (2006).
42. Mecklenbrauker, I., Kalled, S.L., Leitges, M., Mackay, F. & Tarakhovskiy, A. Regulation of B-cell survival by BAFF-dependent PKC δ -mediated nuclear signalling. *Nature* **431**, 456–461 (2004).
43. Steinberg, S.F. Distinctive activation mechanisms and functions for protein kinase C δ . *Biochem. J.* **384**, 449–459 (2004).
44. Yoshida, K. PKC δ signaling: mechanisms of DNA damage response and apoptosis. *Cell. Signal.* **19**, 892–901 (2007).
45. Hartley, S.B. *et al.* Elimination of self-reactive B lymphocytes proceeds in two stages: arrested development and cell death. *Cell* **72**, 325–335 (1993).
46. Hartley, S.B. *et al.* Elimination from peripheral lymphoid tissues of self-reactive B lymphocytes recognizing membrane-bound antigens. *Nature* **353**, 765–769 (1991).
47. Freedman, T.S. *et al.* Differences in flexibility underlie functional differences in the Ras activators son of sevenless and Ras guanine nucleotide releasing factor 1. *Structure* **17**, 41–53 (2009).
48. Kolch, W. Coordinating ERK/MAPK signalling through scaffolds and inhibitors. *Nat. Rev. Mol. Cell Biol.* **6**, 827–837 (2005).
49. Murphy, L.O. & Blenis, J. MAPK signal specificity: the right place at the right time. *Trends Biochem. Sci.* **31**, 268–275 (2006).
50. Philips, M.R. Compartmentalized signalling of Ras. *Biochem. Soc. Trans.* **33**, 657–661 (2005).
51. Daniels, M.A. *et al.* Thymic selection threshold defined by compartmentalization of Ras/MAPK signalling. *Nature* **444**, 724–729 (2006).

ONLINE METHODS

Cell culture. The retroviral packaging ϕ NX-ECO cell line and mouse 3T3 fibroblasts were maintained in DMEM (CellGro) supplemented with 10% (vol/vol) FBS, penicillin, streptomycin and L-glutamine. DT40 cells were maintained in RPMI medium (Gibco) supplemented as described above, as well as with 1% (vol/vol) chicken serum and β -mercaptoethanol (Gibco). *Rasgrp1^{-/-}Rasgrp3^{-/-}* and *Sos1^{-/-}Sos2^{-/-}* DT40 cells have been described³².

Mice. *Prkcd^{-/-}* mice have been described²¹. C57BL/6 and BoyJ mice were from The Jackson Laboratory. Mouse experiments were reviewed and approved by the Institutional Animal Care and Use Committee of the University of California, San Francisco.

Antibodies, reagents and inhibitors. The following antibodies to mouse antigens were used, conjugated to fluorescein isothiocyanate, phycoerythrin, peridinin chlorophyll protein–cyanine 5.5, phycoerythrin–indotricarbocyanine, Pacific blue, allophycocyanin or Alexa Fluor 647: anti-IgD (11-26), anti-IgM (II/41), anti-CD45.1 (A20), anti-CD93 (AA4.1) and anti-CD23 (B3B4; all from eBioscience); anti-CD45.2 (104; Biologend); and anti-CD43 (S7), anti-B220 (RA3-6B2) and anti-CD21 (7G6; all from BD Biosciences). Anti-B220 conjugated to Pacific orange (RM2630) was from Invitrogen. Annexin V conjugated to phycoerythrin was from BD Biosciences and annexin V conjugated to Pacific Blue was from Biologend. DAPI (4,6-diamidino-2-phenylindole) was from Roche. Fluorescein isothiocyanate–conjugated F(ab) monomeric fragment (115-097-020) and goat anti-rabbit IgG conjugated to allophycocyanin (711-136-152) were from Jackson ImmunoResearch Laboratories. Anti-CD16 conjugated to phycoerythrin (MHCD1604) and anti-CD16 conjugated to allophycocyanin (MHCD1605) were from Caltag Laboratories. Antibody to phosphorylated Erk (197G2) or total Erk (9102), anti-RasGRP3 (C33A3) and anti-PKC- δ (2058) were from Cell Signaling; anti-RasGRP1 (m199) was from Santa Cruz; and anti-STIM1 (610954) was from BD. Thapsigargin, Gö6976 and GF-109203X were from Calbiochem. Interleukin 3 (IL-3), IL-6 and stem cell factor (SCF) were from Peprotech or R&D Systems. Lipofectamine 2000 was from Invitrogen. A BrdU labeling kit was used according to the manufacturer's instructions (BD) for labeling with BrdU (5-bromodeoxyuridine).

Plasmids, retroviruses, transfection and infection. Plasmids pDS SP-YFP-STIM1 and pEF-Flag-hDGK- ζ have been described^{13,28}. For transfection of DT40 cells, cells were washed and then resuspended at a density of 6.6×10^7 cells per ml in serum-free RPMI medium. They were transfected by electroporation at 300V for 10 msec with a square-wave electroporator (BTX ECM 800), were allowed to 'rest' for 15 min and were plated in RPMI medium (Gibco) supplemented as described above without antibiotics.

Retroviral constructs for eYFP or eYFP-STIM1 were generated by subcloning of the genes encoding these proteins into the vector MSCV-IThy1.1 by blunt-end ligation. Plasmid pEYFP-N1 (Clontech) was digested with NheI and NotI, plasmid eYFP-STIM1 was digested with NheI and BglII, and the vector was digested with NotI. All digested DNA fragments were made blunt and ligated with a blunt-end ligation kit (Takara). Retroviruses were generated by cotransfection of these constructs with pCL-Eco into ϕ NX-Eco cells with Lipofectamine 2000 according to the manufacturer's instructions (Invitrogen). Supernatants were collected 24 and 48 h after transfection. Then, 3T3 cells were infected with viral supernatants and viral titers were determined by flow cytometry on the basis of the frequency of eYFP-expressing cells. Only supernatants with titers above 1×10^6 particles per ml (with the assumption that every virus infects a cell and a cell does not divide after infection) were used for infection of primary bone marrow cells. For infection, hematopoietic stem cells purified by magnetic-activated cell sorting were incubated overnight in DMEM supplemented with 15% (vol/vol) FCS, IL-3 (20 ng/ml), IL-6 (10 ng/ml) and SCF (100 ng/ml). On day 2, cells were resuspended in viral supernatant supplemented with polybrene (8 μ g/ml), 15% (vol/vol) FCS, IL-3 (20 ng/ml), IL-6 (10 ng/ml) and SCF (100 ng/ml) and were plated in six-well plates. Cells were centrifuged for 2 h at 30 °C and were incubated overnight at 37 °C. The infection was repeated on day 3, and cells were injected into mice on day 4 (as described in the bone marrow–reconstitution section).

Immunoprecipitation, immunoblot analysis and mass spectrometry. DT40 cells at a density of 1×10^7 cells per ml were lysed in 1% (vol/vol) Nonidet-P40 buffer supplemented with protease and phosphatase inhibitors. Sorted bone marrow cells at a density of 5×10^6 cells per ml were lysed. Immunoprecipitation and immunoblot analysis were done essentially as described²⁵. For mass spectrometry, proteins immunoprecipitated with antibody 4G10 were resolved by SDS-PAGE and stained with colloidal blue (Invitrogen), and the band of interest was excised and digested with trypsin. The digestion products were submitted to the Biomolecular Resource Center Mass Spectrometry Facility of the University of California at San Francisco for nano-electrospray liquid chromatography–tandem mass spectrometry and peptide mass fingerprint analyses.

Measurement of intracellular Ca²⁺. Cells were loaded with the fluorescent Ca²⁺ indicator dye Indo-1 according to the manufacturer's instructions (Molecular Probes). Ca²⁺-free and Ca²⁺-bound emissions were measured with a fluorimeter (Hitachi F-4500 or Molecular Devices Flexstation3) during stimulation of the cells. Primary cells were analyzed by multicolor flow cytometry as described⁹.

Intracellular staining of phosphorylated Erk. Primary bone marrow cells were collected on prewarmed serum-free DMEM supplemented with HEPES, pH 7.2, nonessential amino acids, sodium pyruvate, β -mercaptoethanol, penicillin, streptomycin and L-glutamine. Cells were allowed to 'rest' at for 1 h 37 °C in medium containing a nonstimulatory fluorescein isothiocyanate–labeled F(ab) monomeric fragment (1:5,000 dilution), then were stimulated with thapsigargin, fixed for 15 min with prewarmed Cytotfix (BD), washed twice with flow cytometry buffer, and made permeable for 45 min on ice in ice-cold methanol. Cells were then washed three times, were incubated for 45 min in flow cytometry buffer containing antibody to phosphorylated Erk with 4% (vol/vol) mouse serum, were washed twice and then were stained with secondary antibody to rabbit, plus anti-B220 and anti-IgD, and were analyzed by flow cytometry. The same protocol was followed for DT40 cells, except they were stimulated in serum-free RPMI medium supplemented with β -mercaptoethanol and were stained only for phosphorylated Erk (except transiently transfected cells, which were costained for CD16).

Bone marrow reconstitution. Bone marrow cells were collected from donor mice, stem cells were purified with a MACS Lineage Cell Depletion kit (Miltenyi Biotec) and were cultured overnight in DMEM supplemented with 15% (vol/vol) FCS, IL-3 (20 ng/ml), IL-6 (10 ng/ml) and SCF (100 ng/ml). Cells were then infected with retrovirus encoding eYFP or eYFP-STIM1, then were counted and mixed at a ratio of 1:1. Uninfected carrier bone marrow of the same genotype was added to the mixture of infected cells and the cells were then injected into irradiated CD45.2⁺CD45.2⁺ host recipient mice. Bone marrow, spleen and lymph nodes from host recipient mice were collected 8–10 weeks after injection and analyzed by flow cytometry.

Flow cytometry. Single-cell suspensions were prepared from bone marrow, lymph nodes and spleens. Fc receptors were blocked with rat antibody to CD1-CD32 (2.4G2; BD Biosciences). Cells (1×10^6 to 3×10^6) were stained with the appropriate antibodies and were analyzed on a FACSCalibur (BD Biosciences), CyAN ADP (Beckman Coulter), Gallios (Beckman Coulter) or LSR II (BD Biosciences). Forward- and side-scatter exclusion was generally used for the identification of live cells. For analysis of bone marrow chimeras, costaining with DAPI was used for the exclusion of dying cells as well. Data were analyzed with FlowJo software (version 8.8.4; TreeStar). Cells were sorted with a MoFlo system.

Statistical analysis. Error bars were calculated as s.e.m. with n ranging from 3 to 11. P values for comparisons across B cell subsets were calculated with a paired t -test, for which values for each individual mouse were paired. P values for comparisons of different mice (of different genotype) were calculated with an unpaired t -test.